

## Hole states excited by the $^{24}\text{Mg}(p,d)^{23}\text{Mg}$ reaction at 95 MeV

D. W. Miller, W. P. Jones, D. W. Devins, R. E. Marrs,\* and J. Kehayias

*Department of Physics, Indiana University, Bloomington, Indiana 47405*

(Received 15 June 1979)

Experimental excitation energies and angular distributions have been obtained for 33 deuteron groups from the  $^{24}\text{Mg}(p,d)$  reaction at 94.8-MeV bombarding energy with 80-keV experimental resolution. Energies obtained for states in  $^{23}\text{Mg}$  are in agreement with the sixth compilation of Endt and van der Leun up to 7.25 MeV and the recent unpublished ( $p,t$ ) study of Nann *et al.* up to 9.72 MeV. Energies are determined in the present work for 18 additional groups corresponding to excitations between 9.8 and 13.28 MeV. Angular distributions from  $6^\circ$  to  $88^\circ$  laboratory (momentum transfers up to 660 MeV/c) show characteristic oscillatory signatures for  $l = 0$  transitions and broad peaked nonoscillatory behavior for presumed multistep transitions.  $l = 1$  and 2 transitions show a very similar exponential falloff with large momentum transfer, but they can be clearly distinguished by their small-angle behavior after division by an empirical exponential factor or by the dominant momentum transfer dependence from a plane-wave analysis.  $l = 1$  transitions are observed to deep-hole states at 8.91-, 9.02-, 9.67-, and 10.57-MeV excitation. The angular distributions also lead to very probable assignments of  $5/2^-$  and  $7/2^+$  to the 3.97- and 4.68-MeV states of  $^{23}\text{Mg}$ , and are consistent with  $9/2^+$  and  $11/2^+$  assignments to the 2.71- and 5.45-MeV states. Distorted-wave Born approximation (DWBA) predictions using optical potentials from published elastic scattering results show rather good agreement with the shapes of the observed angular distributions for  $l = 2$  transitions, but spectroscopic factors vary by up to a factor of 3 depending on the deuteron potential employed.  $l = 0$  transitions are not fitted in either shape or position of the oscillations, which may be due to the fact that deuteron wave functions derived from elastic scattering are not accurate in the nuclear interior. Reasonable shapes are predicted by preliminary coupled-channel Born approximation (CCBA) analyses for transitions believed to proceed in two steps.

NUCLEAR REACTIONS  $^{24}\text{Mg}(p,d)$ ,  $E = 94.8$  MeV; measured  $\sigma(\theta)$ .  $^{23}\text{Mg}$  levels deduced  $l$ ,  $J$ ,  $\pi$ . S. DWBA analysis, resolution 80 keV,  $\theta = 6^\circ - 88^\circ$ ,  $\Delta\theta = 2^\circ$  or  $4^\circ$ ,  $E_x = 0 - 13.28$  MeV.

### I. INTRODUCTION

One-nucleon pickup reactions provide a unique spectroscopic tool for the examination of single-hole states of nuclei. Of special interest are studies of deep-lying hole states to see if they retain their identity, or whether fragmentation dissolves them to the point that they cannot be recognized in pickup reactions. Such deep states were first investigated with fair to good energy resolution using ( $p,d$ ) reactions at Tokyo<sup>1,2</sup> and Uppsala,<sup>3-6</sup> ( $^3\text{He},\alpha$ ) reactions at Tokyo<sup>7</sup> and Orsay,<sup>8,9</sup> and ( $d,^3\text{He}$ ) and ( $d,t$ ) reactions at Heidelberg,<sup>10,11</sup> Orsay,<sup>12</sup> and Groningen.<sup>13</sup> These and subsequent experiments have shown that pickup spectra can indeed be interpreted roughly in terms of the expectations for hole states from an independent-particle shell model. However, one actually observes experimentally a "quasi-hole" structure, which is broadened and shifted from the mean removal energy predicted by a Hartree-Fock model for a single hole in the target nucleus due to the residual interactions in the final nucleus.<sup>14</sup> Further high-resolution studies to identify the

true nuclear states which share the hole strength seem essential.

The present work represents the first ( $p,d$ ) study with good resolution in the  $s$ - $d$  shell to high excitation of the residual nucleus and to large momentum transfer. States in  $^{23}\text{Mg}$  up to 13.28-MeV excitation were investigated at the Indiana University Cyclotron Facility (IUCF) with about 80-keV overall energy resolution using the  $^{24}\text{Mg}(p,d)^{23}\text{Mg}$  reaction at an average bombarding energy of 94.8 MeV. The ( $p,d$ ) reaction in principle provides an attractive comparison with ( $d,t$ ) and ( $^3\text{He},\alpha$ ) studies because of the longer mean free path of protons and presumed increased sensitivity to the nuclear interior. The choice of proton bombarding energy in this experiment also has some experimental and theoretical advantages over previous cyclotron and linac ( $p,d$ ) studies of  $s$ - $d$  shell nuclei at both lower (27-40 MeV) and higher (156-800 MeV) energies. Deeper-hole states are more accessible at 95-MeV bombarding energy than at the lower energies, and proton distortions in the incident channel are reduced. Further, larger momentum transfers are available

which in principle allow sampling of the higher momentum components of the deuteron and nuclear wave functions. Compared to the higher energy investigations, it was possible to achieve significantly better experimental energy resolution in the present work. In addition, at higher energies the momentum mismatch becomes worse, and above 500 MeV or so  $(p,d)$  reactions may lose their sensitivity to the nuclear interior because of increasing proton absorption. Thus 95 MeV may be about optimum for  $(p,d)$  studies of hole states.

There are a number of questions of interest for possible study by  $(p,d)$  investigations at high-momentum transfer, although a variety of experiments are likely to be required to achieve definitive answers. In addition to utilizing experimental cross sections and asymmetries for  $l$  identification and  $j$  identification of nuclear states, one hopes to achieve quantitative comparisons with nuclear structure calculations of their energies and spectroscopic strengths. These comparisons of course ultimately depend on the utility of the reaction model employed. There is much current interest in the applicability to  $(p,d)$  reactions at higher energies of distorted-wave and coupled-channel calculations,<sup>15-18</sup> which in the past have generally been rather effective in obtaining spectroscopic information from experimental results below 50 MeV. It is important to test a number of aspects of these calculations using  $(p,d)$  reactions at higher momentum transfers, although it is not clear that they can in fact be disentangled. These aspects include the reliability of extraction of spectroscopic factors,<sup>17</sup> the sensitivity to the prescription for the bound-state neutron wave function<sup>19,20</sup> and to high-momentum components of the form factor, the contributions of two-step processes<sup>17,21,24</sup> and their energy dependence, the effects of finite-range and nonlocality corrections,<sup>17,22</sup> the contribution of the deuteron  $D$  state and its momentum transfer dependence,<sup>16</sup> and possible rearrangement effects which might lead to energy-dependent spectroscopic factors.<sup>23</sup> Considerable work has been done on some of these questions recently, but difficulties clearly remain. For example, the Colorado group<sup>16,24</sup> is able to explain the qualitative features of the  $^{12}\text{C}(p,d)^{11}\text{C}$  reaction at bombarding energies of 121 and 700 MeV, with clear evidence for the dominant effect of the deuteron  $D$  state at the higher energy. However, for heavier target nuclei (Ni, Zr, and Pb), there are some unsettling discrepancies with the distorted-wave Born approximation (DWBA) description at 121 MeV.<sup>17,24</sup> At 800 MeV, the spectroscopic factor results for carbon are satisfactory, but for heavier nuclei they deviate by factors of 5–10.<sup>25,26</sup>

Comparison of recent results on Si $(p,d)$  at 95.3 MeV (Refs. 27, 28) and 800 MeV (Ref. 26) show very marked qualitative differences in the observed excitation spectra, suggesting that quite new phenomena are starting to occur as the energy is raised. It seems likely that the 30–200-MeV bombarding energy range available at IUCF covers the beginning of a transition region where  $(p,d)$  studies may be able to sort out the origin of increasing difficulties with distorted-wave approaches as well as the onset of distinctly new phenomena in the pickup process.

The specific choice of targets for initial  $(p,d)$  studies at IUCF of highly excited residual nuclear states was based on several considerations. Earlier work<sup>3-5</sup> on  $s$ - $d$  shell targets showed very prominent high-excitation peaks even under low-resolution conditions, which provided the motivation to study this structure with much better resolution. It was also of interest to initiate  $(p,d)$  investigations with the same  $^{24}\text{Mg}$  and natural Si targets used for concurrent IUCF studies by  $(p,p')$  (Ref. 29) and  $(p,2p)$  (Ref. 30) reactions. Such a program could use common proton optical potentials and determine if common features of the target nuclei, say two-particle two-hole admixtures, might exhibit themselves in the different reaction studies. Extensive nuclear structure calculations also were available for  $A = 23$  (Ref. 31) and  $A = 27$  (Ref. 32) nuclei.

There are of course also disadvantages to the study of  $(p,d)$  reactions on Mg and Si in the 100-MeV range. Both targets exhibit relatively large deformations which present difficulties for theoretical analyses. On the other hand, possible advantages of deformed targets for detailed studies may be the enhancement of two-step effects, the opportunity to examine the results of deformations on inner shells,<sup>33,34</sup> and the effects of phonon-hole coupling.<sup>35-37</sup> Another difficulty with 100-MeV  $(p,d)$  reactions on  $s$ - $d$  shell targets is that they do not exhibit as characteristic orbital angular-momentum transfer signatures as say 52-MeV (Ref. 11) or 80-MeV (Ref. 12, 38, 39)  $(d,^3\text{He})$  and  $(d,t)$  reactions. This may be due to the substantial momentum mismatch of the  $(p,d)$  reaction, or perhaps more likely to the longer mean free path of the proton which allows more partial waves to contribute to the transition amplitude. On the other hand, some other important element of the physics of the process at 100 MeV may be required to explain the clear and characteristic oscillations of  $l=0$  transitions which start to wash out for higher  $l$  transfers.

The present paper reports IUCF results for the  $^{24}\text{Mg}(p,d)^{23}\text{Mg}$  reaction only. Previous  $(p,d)$  studies on Mg targets at proton energies above 20

MeV date back to 1963 with the work of Kavaloski *et al.*<sup>40</sup> at Minnesota at 40 MeV. The first good resolution (95–130 keV) experiments, primarily exciting low states, were those of Kozub<sup>41</sup> at Michigan State and Kunz *et al.*<sup>42</sup> at Colorado, using bombarding energies of 33.6 and 27.3 MeV, respectively. Studies covering the excitation region of <sup>23</sup>Mg up to 60 MeV were carried out at 185 MeV at Uppsala by Källne and Fagerström,<sup>4,5</sup> the later work achieving a resolution of about 260 keV. <sup>24</sup>Mg targets have also been used for several (*d*, *t*) and (*d*, <sup>3</sup>He) investigations above 40-MeV deuteron energy. The high excitation region in the residual nucleus has been studied with good resolution only by Krämer *et al.*,<sup>11</sup> from Heidelberg, at 52 MeV, and very recently at 76 MeV at IUCF by Jacobs *et al.*<sup>38,39</sup> A recent unpublished study of the <sup>25</sup>Mg(*p*, *t*)<sup>23</sup>Mg reaction by Nann *et al.*,<sup>43</sup> at Michigan State, at a bombarding energy of 40 MeV provides excitation energies of states in <sup>23</sup>Mg up to 9.72 MeV, with quoted accuracies of  $\pm 8$  keV or better. Parts of the present <sup>24</sup>Mg(*p*, *d*) investigation have been reported previously<sup>44</sup>; a study of the Si(*p*, *d*) reaction at 95.3 and 135 MeV will be published separately.

Experimental procedures employed in this work will be described in Sec. II. Results obtained for groups observed in this experiment corresponding to excitation energies up to 13.28 MeV, and for angular distributions for the known low-lying  $l=0, 1,$  and  $2$  and possible two-step states, will be presented in Sec. III. Section IV provides empirical  $l$ -transfer and tentative spin and parity assignments for the 3.97-, 4.68-, and 5.45-MeV states, and for the deep-hole states observed in the 8.91- to 10.57-MeV region. DWBA and coupled-channel Born approximation (CCBA) comparisons for the angular distribution shapes for the low-lying states and for relative spectroscopic factors are also presented in Sec. IV.

## II. EXPERIMENTAL PROCEDURE

Protons from the IUCF main cyclotron stage were transported down about 48 m of beam line to the spectrograph experimental area.<sup>45</sup> Data were taken in three separate runs with proton beam energies of 94.5, 94.7, and 95.1 MeV. Momentum-analyzed beam currents on target varied from about 15 to 200 nA, depending on dead-time requirements and accelerator conditions. A  $6.29 \pm 0.3$  mg/cm<sup>2</sup> self-supporting <sup>24</sup>Mg target of 99.94% enrichment was mounted on a multiple-target holder at the center of the 61-cm diameter scattering chamber. The beam spot size on target is normally 1.5–2.5 mm on a side in a nondispersion-matched mode; in the dispersion-matched mode used in this experiment the spot width was typi-

cally increased to about 5 mm. Deuteron spectra were obtained with a quadrupole-dipole-dipole-multipole (QDDM) magnetic spectrograph,<sup>45</sup> with acceptance angle set to  $\pm 17$  mrad horizontally by  $\pm 34$  mrad vertically. The overall resolution for 80-MeV deuterons focused on the helical focal-plane detector<sup>46</sup> was about 80 keV full width at half maximum (a factor of 3 worse than for protons due to aberrations in the higher QDDM field). Particle identification and background reduction were achieved using  $\Delta E$  signals from two Pilot *B* plastic scintillation detectors with thicknesses of 0.64 and 1.27 cm mounted just downstream from the helix. Deuterons were identified on line with software cuts utilizing the data acquisition program DERIVE.<sup>47</sup> Angular distributions were obtained every 2° from 6° to 32° in the laboratory system, and every 4° from 36° to 88°. At forward angles (6° to 48°) a cone-shaped water-cooled Faraday cup was mounted inside the scattering chamber; for overlap angles and angles greater than 24° an external Faraday cup mounted in a beam dump about 6.4 m downstream from the target was used. Since the momentum acceptance of the QDDM spectrograph system is only 3%, three magnetic field settings were required to cover the residual excitation region in <sup>23</sup>Mg up to 12 MeV.

Dead-time corrections were made by using energetic protons detected in an NaI detector (mounted in air at about 20° and 4.5 m from the target) to trigger a pulser which was both scaled directly and fed into the detector outputs for display in the experimental spectrum. Beam intensities were adjusted during runs to maintain the overall dead time measured in this way at 10% or less.

Experimental spectra were analyzed off line using the modified peak-fitting program FITIT,<sup>48</sup> which uses a standard resolved peak shape directly from the data to fit up to five overlapping peaks with variable centroids, peak heights, and widths. Only peaks which were stable in location and width as a function of angle were included in the analysis. For resolved peaks at low excitation, relative cross sections are considered accurate to  $\pm 5\%$ ; this was confirmed by the reproducibility of overlapping runs taken with the same target several months apart. Absolute cross sections for these peaks are believed to be accurate to  $\pm 15\%$ . Somewhat larger absolute errors exist for peaks at higher excitations due to uncertainty in the subtraction of the continuum.

## III. EXPERIMENTAL RESULTS

A composite spectrum for three spectrograph magnetic field settings taken at 8° is shown in

Fig. 1. It should be noted that substantial ( $p, d$ ) strength is observed in the deep-hole state region from 8.91 to 10.57 MeV. Table I lists the excitation energies in  $^{23}\text{Mg}$  corresponding to the deuteron groups observed in the present experiment above 7.2 MeV, which is the upper limit of states included in the compilation of Endt and van der Leun.<sup>49</sup> For each group a comparison is made in the table with the earlier ( $p, d$ ) results of Källne and Fagerström,<sup>5</sup> and with the states reported in the recent higher-resolution  $^{25}\text{Mg}(p, t)$  results of Nann *et al.*<sup>43</sup> States seen in the latter work which do not contribute to the deuteron groups reported here are omitted from the table. Energies quoted by Endt and van der Leun for states below 7.26 MeV agree with those of Nann *et al.* to 13 keV in the worst case, but generally to 4 or 5 keV.

In the present work, excitation energies above 7.2 MeV were determined by calibration against known states from ( $p, d$ ) reactions on  $^{12}\text{C}$ , natural Si, and  $^{24}\text{Mg}$  targets. Energies of states between 11.99 and 13.28 MeV were obtained from an earlier run<sup>27,28</sup> at 135-MeV bombarding energy, where the excitation region from 7 to 13.5 MeV was contained in the spectrum for a single spectrograph field setting. Above 7.2-MeV excitation the 80-keV overall resolution of the present experiment was insufficient to resolve most of the known close-lying states. As would be expected, states are excited with much different strengths in the ( $p, d$ ) reaction at 94.8 MeV from the ( $p, t$ ) reaction at

40 MeV. In general, however, including the effects of resolution, agreement within quoted errors is found between the excitation energies reported in the two experiments up to the limiting excitation investigated by Nann *et al.* Agreement is also found with the earlier ( $p, d$ ) work at 185 MeV.<sup>5</sup>

Angular distributions were measured for 33 of the groups found in this work up to 10.75-MeV excitation. Differential cross sections were obtained at 28 angles between  $6^\circ$  and  $88^\circ$  in the laboratory system for states up to 4.36 MeV, at 22 angles between  $6^\circ$  and  $64^\circ$  for states from 4.68 to 6.54 MeV, and at 11 angles between  $8^\circ$  and  $48^\circ$  for states from 7.79 to 10.75 MeV. For the low-lying states the data cover the momentum transfer range from about 100 to 660 MeV/c.

Figure 2 shows the two known  $l=0$  transitions to states at 2.36 and 4.36 MeV in  $^{23}\text{Mg}$ . The two angular distributions are essentially identical and exhibit the only pronounced oscillations among any of the angular distributions for known states obtained at this bombarding energy. Three known  $l=1$  transitions are displayed in Fig. 3. The observed group corresponding to 2.77-MeV excitation shows a small but distinct energy shift to higher laboratory energy at larger angles, caused by an unresolved contribution from the known state at 2.71 MeV. Since the latter state may be  $\frac{3}{2}^+$ , and is certainly even parity,<sup>49</sup> the angular distribution shown in Fig. 3 for the 2.77-MeV state is not pure  $l=1$  at the backward angles. A weak  $l=2$  transition

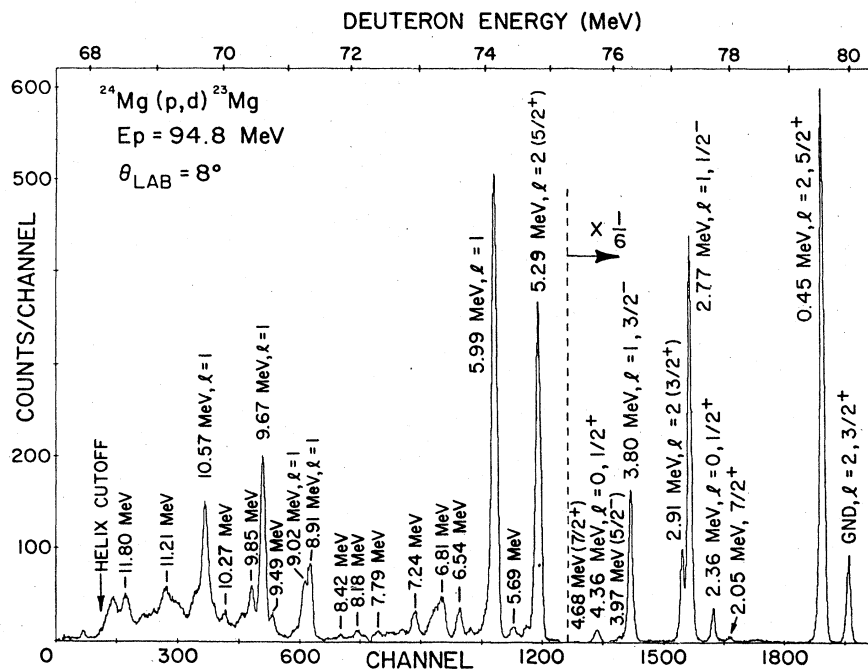


FIG. 1. A composite  $^{24}\text{Mg}(p,d)^{23}\text{Mg}$  spectrum obtained by combining spectra for three different magnetic field settings at the same laboratory angle of  $8^\circ$ . Note the vertical scale change at channel 1300.

TABLE I. Groups studied in this experiment corresponding to excitation energies in  $^{23}\text{Mg}$  above 7.2 MeV.

Present work: $^{24}\text{Mg}(p, d)$ $E_p = 94.8$ MeV		$^{25}\text{Mg}(p, t)^a$ $E_p = 40$ MeV	$^{24}\text{Mg}(p, d)^b$ $E_p = 185$ MeV
$E_x$ (MeV)	Assignment	$E_x$ (MeV)	$E_x$ (MeV)
7.24 ± 0.02	c	7.231 ± 0.007 7.259 ± 0.007	7.24 ± 0.06
7.42 ± 0.03	c	7.381 ± 0.008 7.444 ± 0.008 7.493 ± 0.008	
7.61 ± 0.03	c	7.582 ± 0.006 7.621 ± 0.008	
7.79 ± 0.03	(2 step + $l=1$ )	7.780 ± 0.006 [7.795 ± 0.006] <sup>d</sup> 7.852 ± 0.006	7.73 ± 0.06
8.06 ± 0.04	c	8.016 ± 0.006 8.058 ± 0.007 8.076 ± 0.008	
8.18 ± 0.03	c	8.155 ± 0.006 8.193 ± 0.008	8.17 ± 0.07
8.42 ± 0.04	c	8.393 ± 0.006 8.420 ± 0.006 8.453 ± 0.005	
8.61 ± 0.04	c	8.557 ± 0.006 8.617 ± 0.006	
8.77 ± 0.05		8.758 ± 0.006 8.793 ± 0.008	
8.91 ± 0.02	$l=1$	8.870 ± 0.008 8.916 ± 0.006 8.941 ± 0.007	8.95 ± 0.06
9.02 ± 0.03	$l=1$	8.990 ± 0.006 9.018 ± 0.006	
9.14 ± 0.04	(2 step)	9.103 ± 0.006 9.138 ± 0.006	
9.49 ± 0.04	( $l=0 + l=1$ or 2)	9.465 ± 0.006	
9.67 ± 0.02	$l=1$	9.596 ± 0.008 9.642 ± 0.008 9.662 ± 0.008 9.717 ± 0.008	9.68 ± 0.10
9.75 ± 0.05	c		
9.85 ± 0.03	( $l=2$ )		
9.97 ± 0.04	(2 step + $l=1$ )		
10.12 ± 0.05	(2 step)		
10.27 ± 0.03	(2 step + $l=1$ )		
10.44 ± 0.05	(2 step + $l=1$ )		
10.57 ± 0.02	$l=1$		10.55 ± 0.11
10.75 ± 0.04	(2 step + $l=2$ )		
10.92 ± 0.07	c		
11.03 ± 0.06	c		
11.21 ± 0.06	c		
11.38 ± 0.06	c		
11.54 ± 0.06	c		

TABLE I. (Continued)

Present work: $^{24}\text{Mg}(p,d)$ $E_p = 94.8$ MeV		$^{25}\text{Mg}(p,t)^a$ $E_p = 40$ MeV	$^{24}\text{Mg}(p,d)^b$ $E_p = 185$ MeV
$E_x$ (MeV)	Assignment	$E_x$ (MeV)	$E_x$ (MeV)
$11.80 \pm 0.04$	c		
$11.99 \pm 0.05$	c		
$12.48 \pm 0.08$	c		
$12.69 \pm 0.08$	c		
$12.94 \pm 0.08$	c		
$13.28 \pm 0.08$	c		

<sup>a</sup>Selected states from Ref. 43.<sup>b</sup>Reference 5.<sup>c</sup>Angular distribution not extracted.<sup>d</sup> $\frac{5}{2}^+$ ,  $T = \frac{3}{2}$  state according to Ref. 49, should not contribute appreciably in the present work.

to a state at 3.86 MeV is also not resolved from the group observed for the 3.80-MeV state in Fig. 3, but its contribution is believed to be very small. A similar remark applies to a state with unknown

assignment at 5.93 MeV, 54 keV below the strong 5.99-MeV  $l = 1$  group.

The four known  $l = 2$  transitions shown in Fig. 4 exhibit very little angular structure, but the cross

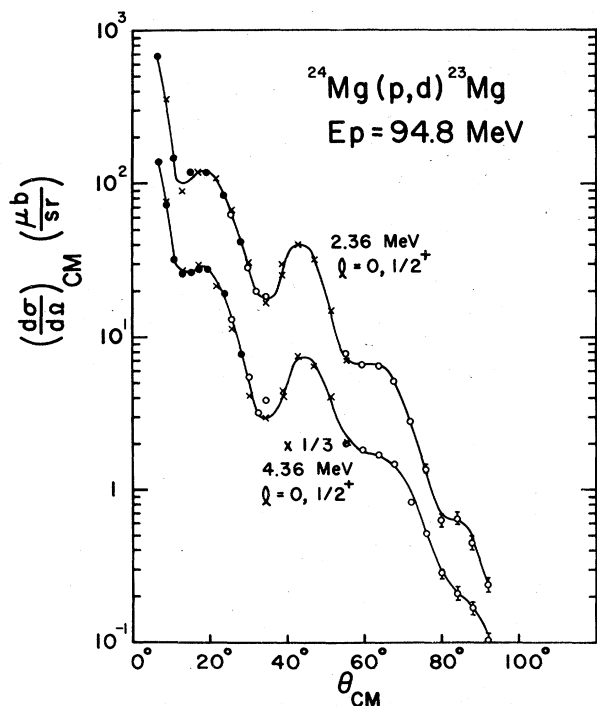


FIG. 2. Angular distributions obtained for the two known  $l = 0$  transitions to low-lying states in  $^{23}\text{Mg}$  at 2.36 and 4.36 MeV. The three different sets of symbols represent results obtained with the same target in separate runs one to two months apart without normalization. Errors shown are purely statistical, and the curves are guides to the eye. Note the factor of  $\frac{1}{3}$  by which the cross sections for the 4.36-MeV state were multiplied before plotting.

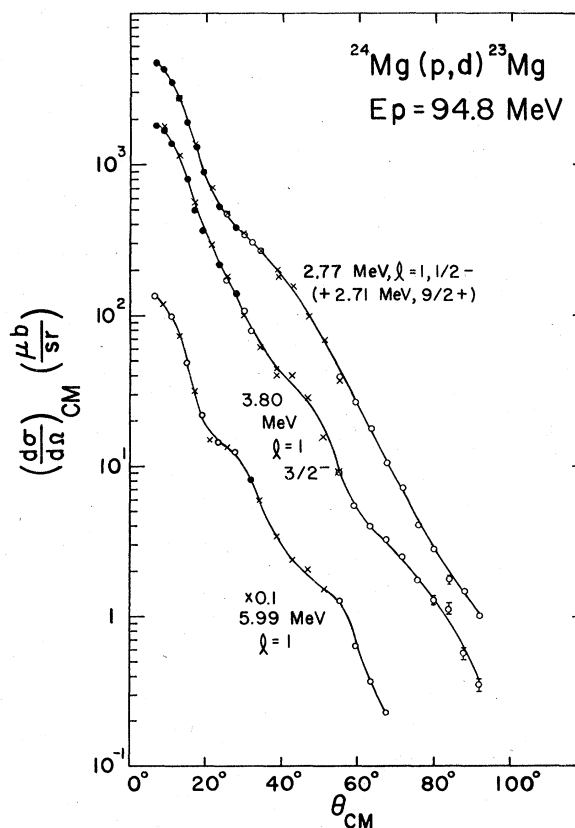


FIG. 3. Angular distributions for the three known  $l = 1$  transitions to low-lying states in  $^{23}\text{Mg}$  at 2.77, 3.80, and 5.99 MeV. The 2.77-MeV state is not resolved from a weaker  $\frac{3}{2}^+$  state at 2.71 MeV (see text). Symbols, curves, and plotting factors are explained in the caption for Fig. 2.

sections do start to turn down at  $6^\circ$  laboratory in contrast to the  $l=1$  cases. This does not appear from the figure to be true for the 2.91-MeV group, but it is not completely resolved from the tail of the very strong 2.77-MeV  $l=1$  group.

At the top of Fig. 5 is plotted the angular distribution obtained for the  $\frac{7}{2}^+$  2.05-MeV state in  $^{23}\text{Mg}$ . This state is generally believed to be excited by a two-step mechanism in the  $(p,d)$  reaction, since two-particle two-hole components of the  $^{24}\text{Mg}$  ground state are not expected to contain enough  $(1g_{7/2})^2$  to allow direct one-step pickup with the observed cross section. Similar angular distributions are shown in Fig. 5 for the 3.97- and 4.68-MeV states, which also likely proceed by two-step processes. Also plotted is the very weak 5.45-MeV group, which may go by a multistep transition.

A summary of the characteristic features of the angular distributions observed for known  $l=0, 1,$  and  $2$  transitions, as well as the probable two-step

transition to the  $\frac{7}{2}^+$  state at 2.05 MeV, is given in Fig. 6. As mentioned earlier it is clear from this figure that the  $l$  selectivity for  $(p,d)$  reactions on  $s-d$  shell targets at 94.8 MeV is not so characteristic as for lower energy  $(p,d)$  and  $(d,t)$  reactions, particularly in distinguishing between  $l=1$  and  $l=2$  transitions. This is important to the identification of the deep-hole states discussed in Sec. IVA 2.

Angular distributions for a number of weaker groups in the region of  $^{23}\text{Mg}$  excitation from 5.69 to 7.79 MeV are shown in Fig. 7. These distributions are subject to much greater uncertainties than those in the previous figures, a consequence of their low cross sections and the higher density of states. Most of the groups shown contain contributions from unresolved states, which presumably accounts for their nonstandard shapes compared to Fig. 6. Similar remarks apply to the angular distributions for most of the groups corresponding to the excitation region from 8.77 to

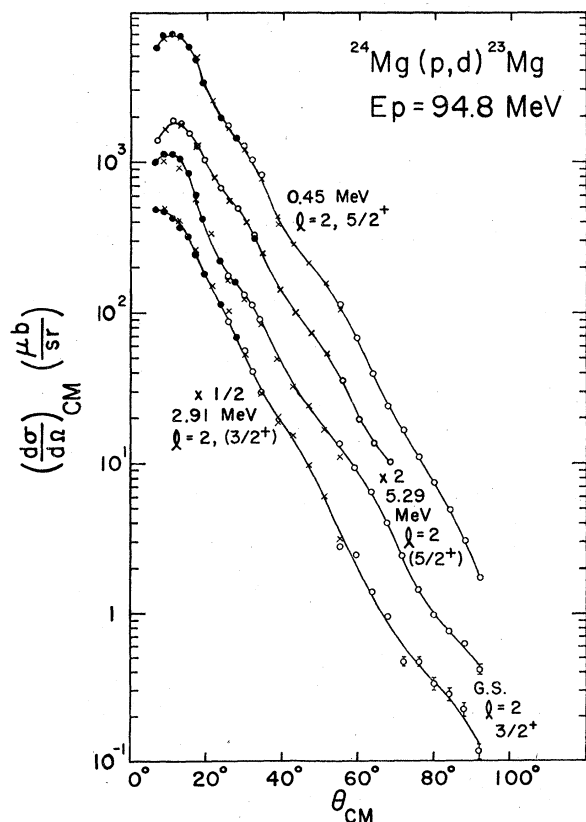


FIG. 4. Angular distributions obtained for the four known  $l=2$  transitions to the ground state and low-lying states in  $^{23}\text{Mg}$  at 0.45, 2.91, and 5.29 MeV. There may be an unresolved  $l=1$  contribution to the 2.91-MeV state (see text). Symbols, curves, and plotting factors are explained in the caption for Fig. 2.

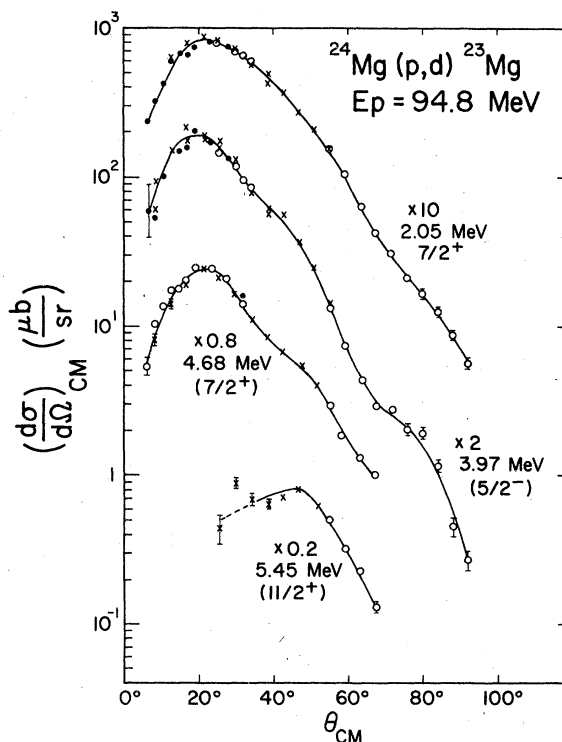


FIG. 5. Angular distributions for the  $\frac{7}{2}^+$  2.05-MeV state, and for the 3.97, 4.68, and 5.45-MeV states whose spin and parity assignments are discussed in Sec. IV A of the text. All four angular distributions are indicative of multistep or  $l > 2$  transitions, or of interference between such transitions. Symbols, curves, and plotting factors are explained in the caption for Fig. 2.

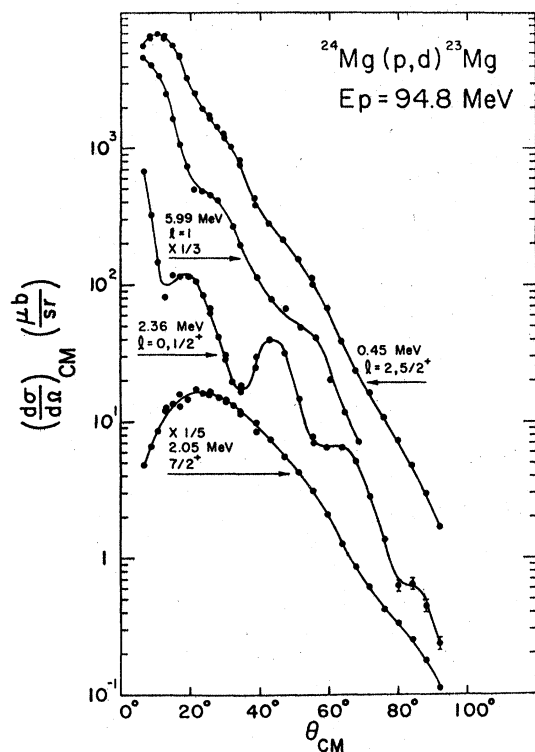


FIG. 6. A comparison of typical known angular distributions taken from Figs. 2-5 to illustrate the characteristic signatures of different  $(p, d)$  orbital angular momentum transfers at 94.8 MeV. The curves are guides to the eye.

10.75 MeV shown in Fig. 8. Among these groups it is unlikely that single states contribute to the extracted angular distributions, except possibly in the case of the very strong groups (see Fig. 1).

#### IV. DISCUSSION OF RESULTS

##### A. Empirical conclusions

##### 1. States at medium excitations

Accurate excitation energies and definite (or alternate) spin and parity assignments for the low-lying states of  $^{23}\text{Mg}$  are given in the recent compilation of Endt and van der Leun.<sup>49</sup> The lowest state for which a definite spin and parity assignment is not made by these authors is at 2.71 MeV. This state is not resolved in the present work from the 2.77-MeV state, but the energy shift of the centroids of the observed group implies an increasing contribution of the 2.71-MeV state at larger angles. Such a behavior would be consistent with the  $\frac{3}{2}^+$  assignment for the 2.71-MeV state indicated by Endt and van der Leun (presumably requiring a two-step process), but not with the

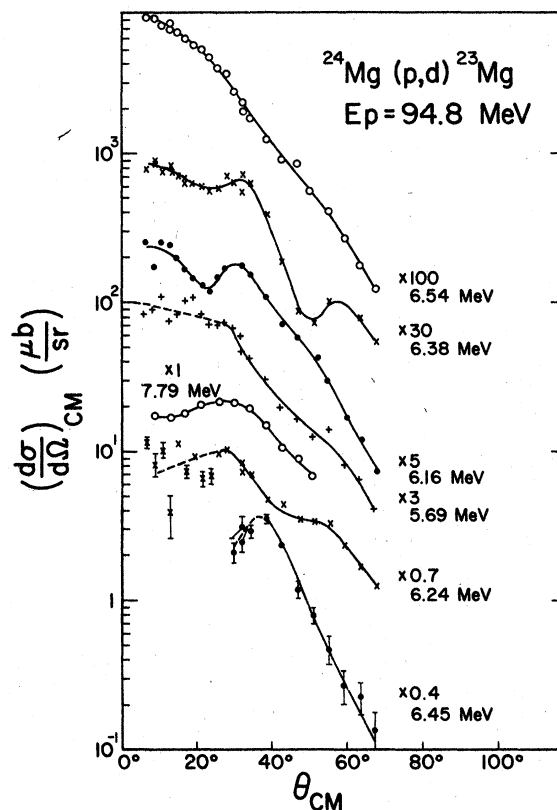


FIG. 7. Angular distributions for deuteron groups corresponding to excitations in  $^{23}\text{Mg}$  from 5.69 to 7.79 MeV. Errors, curves, and plotting factors are explained in the caption for Fig. 2.

possible alternate  $\frac{5}{2}^+$  assignment.

The first state for which no assignment is quoted<sup>49</sup> is at 3.97 MeV. This state and the next lower state at 3.86 MeV are believed<sup>50</sup> to be the (inverted) mirror states of the  $\frac{5}{2}^-$  3.85- and  $\frac{5}{2}^+$  3.91-MeV states in  $^{23}\text{Na}$ . An  $l=2$  transition reported by Nelson and Roberson<sup>50</sup> to the 3.86-MeV state in  $^{23}\text{Mg}$  provides a  $\frac{3}{2}^+$  or  $\frac{5}{2}^+$  assignment. This group could not be resolved in the present work from the tail of the much stronger  $l=1$  group leading to the 3.80-MeV state. However, the angular distribution shown in Fig. 5 for the 3.97-MeV state is certainly not consistent with an  $l=2$  transfer, and likely suggests a two-step mechanism. This would be required for a  $\frac{5}{2}^-$  assignment, unless a two-particle two-hole component involving  $(1f_{5/2})^2$  in the  $^{24}\text{Mg}$  ground state is appreciable. In the latter event the angular distribution for the 3.97-MeV state could represent a one-step  $l=3$  pickup (see Sec. IV B for the corresponding DWBA prediction) or interference between this and a two-step mechanism. Either way, the shape of the angular distribution strongly favors the empirical assignment of  $\frac{5}{2}^-$  rather than  $\frac{5}{2}^+$  to the 3.97-MeV state,



in agreement with an inversion of the 3.86–3.97-MeV states in  $^{23}\text{Mg}$  from the mirror states in  $^{23}\text{Na}$ .

The next uncertain state<sup>49</sup> in  $^{23}\text{Mg}$  is at 4.68 MeV. It has been proposed that this state is  $\frac{7}{2}^+$ , based upon Nilsson model arguments and experimental results.<sup>50,51</sup> A definite  $\frac{7}{2}^+$  assignment has been made to the presumed mirror state at 4.78 MeV in  $^{23}\text{Na}$ . A  $\frac{7}{2}^+$  assignment for the 4.68-MeV state in  $^{23}\text{Mg}$  is empirically quite consistent with the similarity of the first and third angular distributions in Fig. 5.

The next unassigned<sup>49</sup> state in  $^{23}\text{Mg}$  is at 5.45 MeV; it has been proposed<sup>50</sup> to have spin and parity  $\frac{11}{2}^+$ . The very weak group observed in the present experiment which corresponds to this state rides on the tail of the strongly forward-peaked  $l=2$  5.29-MeV group, so that large errors result in extracting cross sections at forward angles as shown at the bottom of Fig. 5. It is clear that the cross section for this group holds up to about 50° c.m., whereas the 5.29-MeV group

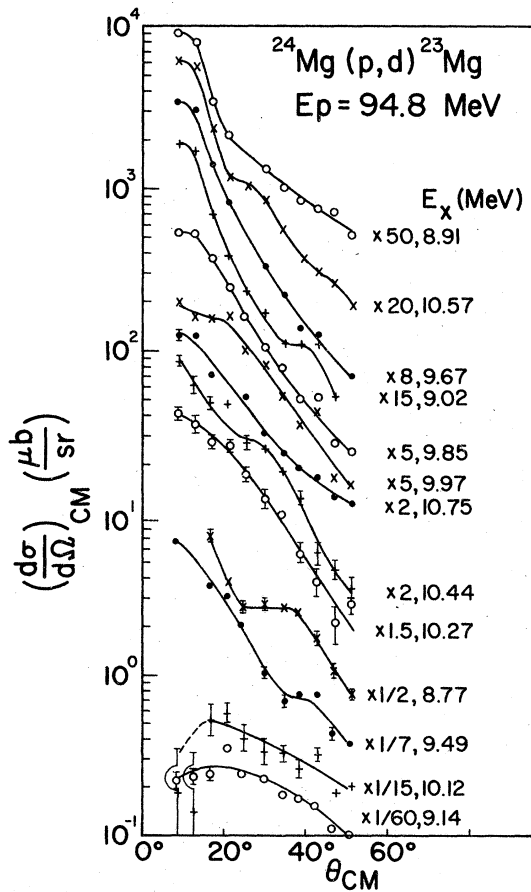


FIG. 8. Angular distributions obtained for deuteron groups corresponding to the deep-hole state region from 8.77 to 10.75-MeV excitation. Errors, curves, and plotting factors are explained in the caption for Fig. 2.

is dropping rapidly over this angular range. The resulting shape of the angular distribution for the 5.45-MeV group in Fig. 5 then suggests either a two-step process or an  $l$  transfer considerably greater than 2. In the mirror nucleus  $^{23}\text{Na}$  the only nearby state which could not be reached by  $l=2$  is the 5.53-MeV state which is assigned<sup>49</sup>  $\frac{11}{2}^+$ . It is highly unlikely that even the small 4- $\mu\text{b}/\text{sr}$  peak cross section observed in this work for the 5.45-MeV state in  $^{23}\text{Mg}$  could result from a one-step  $1i_{11/2}$  pickup from a small component of the  $^{24}\text{Mg}$  ground state, so a multistep transition of some sort is probable. Either way, however, the shape of the angular distribution for the 5.45-MeV state is empirically more consistent with an  $\frac{11}{2}^+$  assignment than with any other assignment appearing among nearby mirror  $^{23}\text{Na}$  states.

Little can be concluded about the angular distributions shown in Fig. 7 because of the low intensities of the groups and the close proximity of the states. The angular distributions of the groups corresponding to excitations of 5.69 MeV (unresolved 5.69+5.71-MeV states), 6.16 MeV (6.13+6.19-MeV states), 6.24 MeV (with some tail from the 6.19-MeV state), and 6.54 MeV (6.51+6.54+6.57-MeV states) look like mixtures of  $l=1$  or 2 and two-step transitions. Forward-angle cross sections could not be extracted for the 6.45-MeV group. It would be tempting to interpret the rather unusual oscillation of the 6.38-MeV group as due to an  $l=0$  transition to a  $\frac{1}{2}^+$  state corresponding to the  $\frac{1}{2}^+$  6.31-MeV state in the mirror nucleus  $^{23}\text{Na}$ . However, by comparison with the observed shift between the first two  $\frac{1}{2}^+$  states in  $^{23}\text{Mg}$  and  $^{23}\text{Na}$ , and with the shell-model predictions,<sup>31</sup> one would expect the third  $\frac{1}{2}^+$  state to lie lower than 6.31 MeV in  $^{23}\text{Mg}$ . Furthermore, the maxima and minima in the oscillations in the angular distribution of the 6.38-MeV group are shifted from the observed oscillations for the first two known  $l=0$  transitions even more than the DWBA prediction (see Sec. IV B).

The 7.79-MeV group has an angular distribution in Fig. 7 which suggests a two-step process for the dominant 7.78-MeV state, with possibly some  $l=1$  contribution from the 7.85-MeV state (see Table I). There are a number of states with unknown assignments in the mirror nucleus  $^{23}\text{Na}$  in this region; in fact, nearly half again as many as observed by Nann *et al.*<sup>43</sup> in  $^{23}\text{Mg}$ . The  $\frac{5}{2}^+$   $T=\frac{3}{2}$  state at 7.79 MeV (Ref. 49) is centered on the group observed in this experiment, but should not contribute appreciably because it is isospin forbidden.

## 2. Deep-hole states

It is clear from Fig. 6 that there is not a marked difference between  $l=1$  and  $l=2$  angular distribu-

tions at this bombarding energy, both showing modest structure superimposed on an exponential decrease of a few orders of magnitude out to  $90^\circ$  c.m. In spite of the pronounced peaks due to presumed deep-hole states shown in Fig. 1, the cross sections in this region of excitation are not large, and data were therefore taken at fewer angles in this region. In order to aid in the identification of the deep-hole state  $l$  transfers, two methods of display of the data were utilized in addition to Fig. 8 to emphasize the differences between  $l=1$  and  $l=2$  transitions.

As a first empirical approach, the data for all known  $l=1$  and  $l=2$  transfers were replotted as a function of momentum transfer  $q$  in MeV/c after division by an exponential factor of the form  $\exp(-q/66)$ . The original motivation for this display was to emphasize small oscillatory differences, although the suggestion has been made<sup>52</sup> that both the nuclear form factor and the one-particle momentum distribution in a nucleus may in fact have an exponential dependence on momentum transfer  $q$  for  $q$  large but  $q/A$  not large (where  $A$  = nuclear mass number). The exponential factor chosen was based upon an average representation of the observed decrease in cross section for the known  $l=1$  and  $l=2$  transitions. Figure 9 displays by solid curves the results obtained in this way for known states. This representation clearly emphasizes the difference of the forward-angle behavior, where all known  $l=1$  transfers peak between 110–120 MeV/c and all known  $l=2$  transfers peak between 145–165 MeV/c. (Note that the 2.91-MeV group peaks a little forward of the other  $l=2$  cases, but it is believed to have some  $l=1$  contamination as discussed in Sec. III.) The display in Fig. 9 also emphasizes backward-angle structure, but unfortunately it appears that one cannot draw definite conclusions about either  $l$  or  $j$  dependence by examining this representation at large momentum transfers. It is likely that the display overemphasizes experimental errors in the small cross sections at the large angles. (One should again note that the observed group corresponding to the 2.77-MeV state appears to contain a two-step contamination which affects the shape of this group at large angles.)

All curves in Fig. 9 are arbitrarily normalized so that they may be reasonably displayed and compared on one graph. The results obtained for five of the deep-hole states are shown by experimental points connected by dashed curves. From the locations of the first apparent maxima one can make empirical orbital angular momentum assignments of  $l=1$  for the 8.91-, 9.02-, 9.67-, and 10.57-MeV deep-hole states. These four assignments have been confirmed recently using the

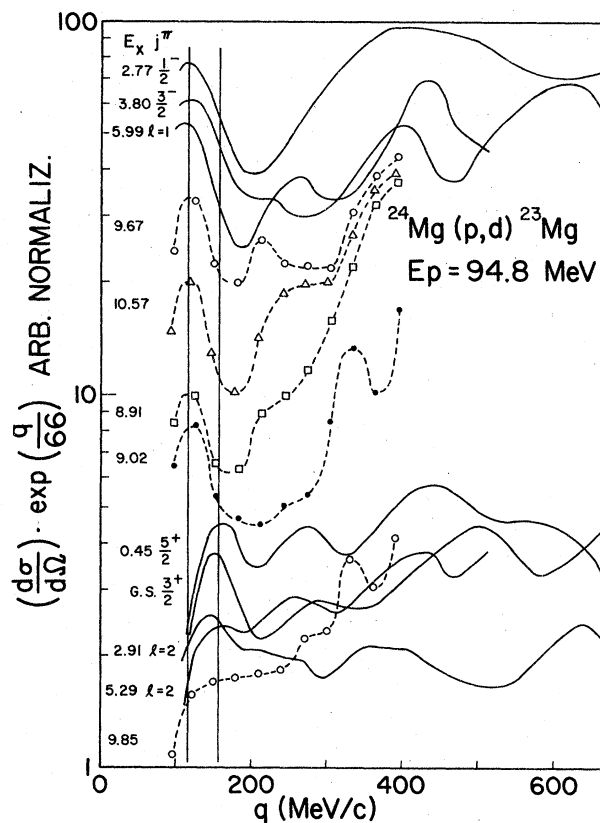


FIG. 9. Display of angular distributions after division by an exponential momentum-transfer factor. Solid curves are obtained from the guides to the eye for known  $l=1$  and  $l=2$  transitions to low-lying states in Figs. 3 and 4. Dashed curves guide the eye between data points obtained for deep-hole states. The vertical reference lines are drawn at 115 MeV/c and 155 MeV/c.

$^{24}\text{Mg}(d,t)^{23}\text{Mg}$  reaction at 76 MeV,<sup>38,39</sup> and are in agreement with an earlier assignment to two states quoted at 9.68 and 10.55 MeV using the  $^{24}\text{Mg}(p,d)^{23}\text{Mg}$  reaction at 185 MeV.<sup>5</sup>

On the other hand, Fig. 9 shows that a weak group corresponding to an excitation of 9.85 MeV in  $^{23}\text{Mg}$  definitely is not  $l=1$ , in agreement with the recent  $(d,t)$  results.<sup>38,39</sup> No firm assignments can be made to weaker groups found in this region, although some suggestions based on the angular distributions in Fig. 8 are given in parentheses in Table I.

As a second approach, an attempt was made to develop a representation of the data which would remove the rapid angular dependence of the cross sections on a theoretical basis. Although full DWBA calculations will be discussed in the next section, there was hope that a plane-wave approximation might give some understanding of the underlying physics behind the effects which show up in the detailed DWBA fits. A standard plane-

wave analysis,<sup>53</sup> using a cutoff due to strong deuteron absorption, leads to an expression for the differential cross section for the pickup of a neutron with orbital angular momentum  $l_n$  which is of the form  $(q^2 + \kappa^2)^{-2}$  times the square of the difference of Bessel functions  $J_{l_n}(qR)$  and  $J_{l_n+1}(qR)$ , with appropriate factors. In this expression  $\kappa$  is determined from the neutron separation energy  $E_s$  and mass  $M_n$  by  $E_s = (\hbar^2 \kappa^2)/(2M_n)$ ,  $q$  is the momentum transfer, and the cutoff radius  $R$  is chosen on the decaying tail of the bound-neutron wave function. The term involving  $J_{l_n+1}(qR)$  is multiplied directly by the momentum transfer, which enhances the importance of this term compared to low-energy stripping and pickup reactions. Figure 10 shows the results using  $R = 1.33 A^{1/3}$  fm in this model for  $l = 0, 1$ , and  $2$  transitions, plotted as  $(q^2 + \kappa^2)^2 (d\sigma/d\Omega)$  in order to remove the momentum dependence of the leading factor. Also plotted are experimental cross sections for three corresponding known states, also multiplied by  $(q^2 + \kappa^2)^2$ . The choice  $R = 1.33 A^{1/3}$  fm gives a good fit to the first observed maximum for the known  $l = 0, 2$  and probably  $1$  transitions, and also reproduces subsequent  $l = 0$  maxima and minima satisfactorily, although shifting of subsequent  $l = 1$  and  $2$  maxima is apparent. Clearly a  $(q^2 + \kappa^2)^{-2}$  momentum dependence cannot mock up the actual exponential dependence found experimentally over the full range, but it does remove much of the initial drop-off and has some theoretical basis. The most useful result is the clear  $l$  identification provided by the first observed maximum in the plane-wave approach, just as observed in the empirical approach which removed an exponential factor. Since the conclusions for the deep-hole states based on the first observed maxima are the same, the experimental results in Fig. 9 are not replotted in the format of Fig. 10.

#### B. DWBA and CCBA comparisons

DWBA calculations using the distorted-wave code<sup>54</sup> DWUCK4 have been carried out in an attempt to provide quantitative comparisons with the observed angular distributions for the known low-lying states and to extract spectroscopic information. The proton potentials used were based on the work of Nadasen *et al.*,<sup>55</sup> while a variety of deuteron potentials have been tried (Kiss *et al.*,<sup>56</sup> Duhamel *et al.*,<sup>57</sup> and an adiabatic potential following Johnson and Soper<sup>58</sup>). Finite-range and nonlocality effects were treated approximately in the calculations. Form factors were calculated using the separation-energy prescription with a Woods-Saxon radius of  $1.25 A^{1/3}$  fm and a diffuseness of  $0.65$  fm.

For the  $l = 2$  calculations, reasonably good fits

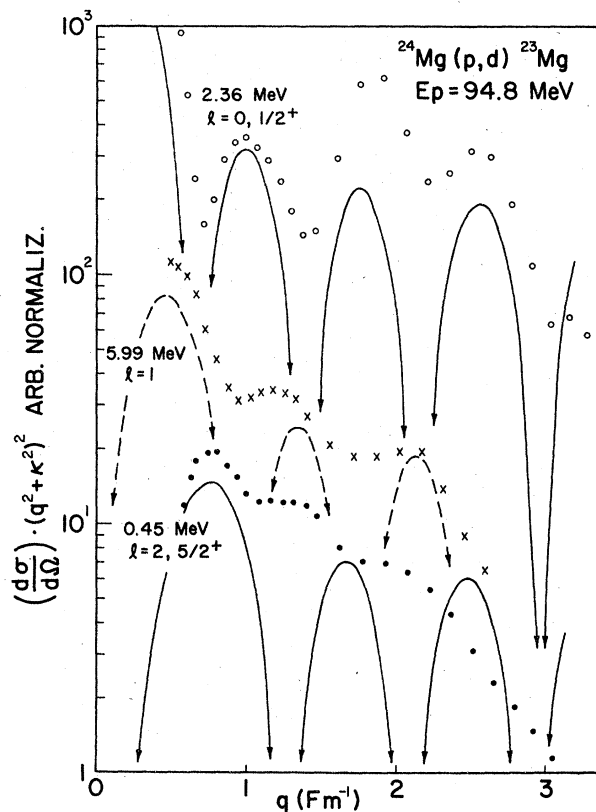


FIG. 10. Standard plane-wave cutoff model predictions (solid and dashed curves) multiplied by  $(q^2 + \kappa^2)^2$  as discussed in text for  $l = 0, 1$  and  $2$  transitions. Comparison points are taken from smooth curves through the experimental data for sample transitions in Figs. 2 to 4. Vertical scales are arbitrarily normalized for convenience of the comparison display.

are obtained to the general slope of the cross sections with angle regardless of the deuteron potentials used, as illustrated in Fig. 11 for the  $0.45$ -MeV state. Even though there are not marked differences in the shapes predicted using the four different deuteron potentials, there is up to a factor of 3 difference in the extracted absolute spectroscopic factors. An uncertainty also probably arises from the separation-energy prescription used in the calculation of the form factor.<sup>36</sup> An analysis of these  $l = 2$  DWUCK calculations showed very little contribution from the nuclear interior to the predicted cross section at the first maximum at  $10^\circ$  c.m., with nearly all of the contribution coming from outside  $1.25 A^{1/3}$  ( $= 3.6$ ) fm.

Figure 12 shows the experimental results compared to the DWUCK prediction for the  $l = 1$  transition to the  $5.99$ -MeV state and the  $l = 0$  transition to the  $2.36$ -MeV state, both using the deuteron potential from Ref. 56. The predictions are normalized at forward angles to the experimental

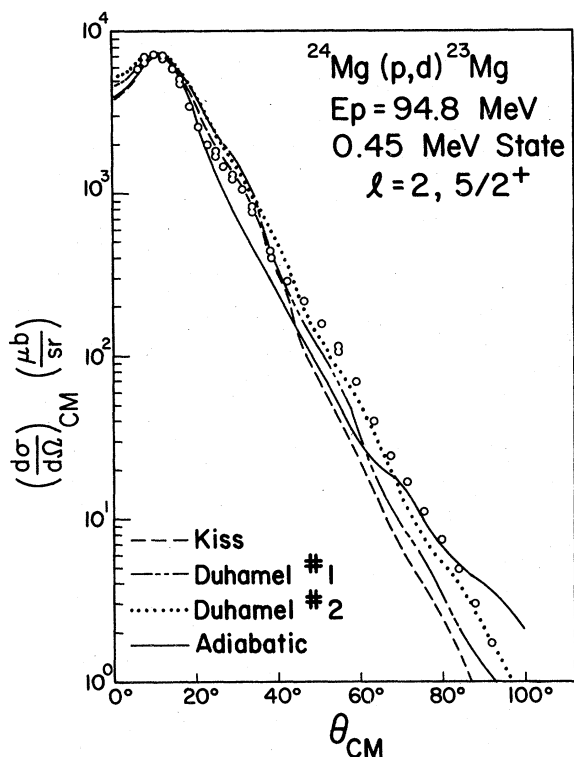


FIG. 11. Comparison of experimental data with DWBA predictions for  $1d_{5/2}$  transfer to the 0.45-MeV state of  $^{23}\text{Mg}$  for four different choices of deuteron potentials described in the text. All theoretical curves are normalized to the first maximum for comparison purposes, but spectroscopic factors vary considerably.

results for the best comparison. Oscillations predicted for the  $l=1$  transition are roughly in phase with those shown by the data, but the general slope is not well reproduced, and the overall fit is inferior to those shown for the  $l=2$  transition in Fig. 11.

The  $l=0$  predictions clearly do not provide a good fit to the shape of the experimental angular distributions, as shown in Fig. 12. Predicted oscillations have roughly the correct angular spacing, but the average slope is not well reproduced and the maxima and minima are shifted to larger angles than those exhibited by the data. Similar problems have been observed for the reactions  $^{24}\text{Mg}(p,d)^{23}\text{Mg}$  investigated at 27.3 MeV (Ref. 42) and  $^{24}\text{Mg}(d,^3\text{He})^{23}\text{Na}$  at 52 MeV,<sup>11</sup> where different radius prescriptions were needed to obtain  $l=0$  fits. In the present work the radius and diffuseness of the form factor for the  $l=0$  transitions were varied over the range from  $1.10 A^{1/3}$  to  $1.40 A^{1/3}$  fm and 0.5 to 0.8 fm, respectively. These adjustments did not make substantial improve-

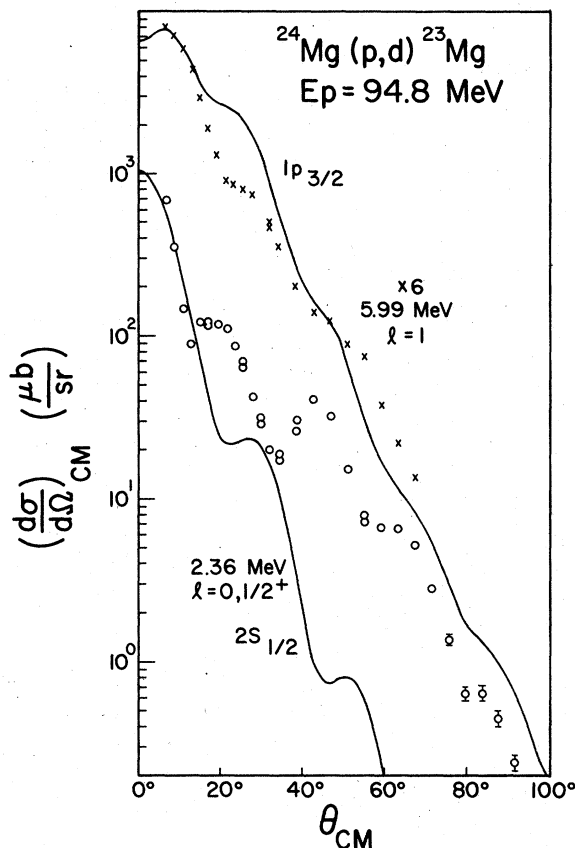


FIG. 12. Comparison of experimental data with normalized DWBA predictions for  $2s_{1/2}$  and  $1p_{3/2}$  transfers to the 2.36- and 5.99-MeV states of  $^{23}\text{Mg}$  using the deuteron potential of Ref. 56.

ments to the  $l=0$  fits. The rms radius prescription<sup>59</sup> for the neutron orbit was not tried. An analysis of these  $l=0$  DWUCK calculations showed that a substantial contribution to the predicted  $0^\circ$  cross section comes from the interior radial region between 0.5 and 2.0 fm, although the major contribution is still from the region beyond 3.6 fm.

It is interesting to note that the simple plane-wave analysis shown in Fig. 10 with a cutoff radius of  $1.33 A^{1/3}$  fm does predict the first experimental maximum for  $l=0$ , 2, and probably 1 transitions, while the presumed more realistic DWUCK predictions fit the first experimental maximum for  $l=2$  and probably  $l=1$  but not for  $l=0$ . It should be emphasized that no attempt was made to include possible two-step interference effects in the one-step allowed transitions.

Some preliminary coupled-channel analyses using the CCBA code CHUCK<sup>54</sup> have been attempted for two of the states which are not likely to be populated by one-step pickup. The two-step prediction for inelastic excitation of the lowest  $2^+$

state in  $^{24}\text{Mg}$  followed by  $1d_{5/2}$  neutron pickup to excite the  $\frac{7}{2}^+$  state at 2.05 MeV in  $^{23}\text{Mg}$  is shown as a dashed curve in Fig. 13, with normalization to fit the experimental data. Other possible two-step paths were not included in the calculation. Purely for comparison, a DWUCK prediction (using the deuteron potential of Ref. 56) for the unlikely one-step  $l=4$  pickup from a two-particle two-hole component in the  $^{24}\text{Mg}$  ground state involving  $(1g_{7/2})^2$  is shown by a solid curve. For this comparison the DWUCK prediction for a one-step transition to the 2.05-MeV state corresponds to a spectroscopic factor of about 0.03. Both the DWBA and CCBA predictions peak at about the right angle, but fall off too rapidly at larger angles.

Figure 13 also shows the experimental angular distribution for the 3.97-MeV state, whose spin and parity are likely  $\frac{5}{2}^-$  as discussed in Sec. IV A. Superimposed are the normalized DWBA prediction (using the deuteron potential of Ref. 56) for a possible one-step  $1f_{5/2}$  pickup (solid curve), and a preliminary normalized CCBA prediction for a two-step process with inelastic excitation of the lowest  $2^+$  state in  $^{24}\text{Mg}$  followed by  $1p_{1/2}$  neutron pickup only (dashed curve). The one-step process corresponds to an absolute spectroscopic factor of about 0.02. Again both predictions peak at about the correct angle but drop off too rapidly thereafter.

Evidence for an  $\frac{11}{2}^+$  assignment for the 5.45-MeV state, excited weakly in this experiment, was given in Sec. IV A. A normalized DWBA prediction, assuming a (highly unlikely) one-step  $1i_{11/2}$  pickup, is shown by the solid curve at the bottom of Fig. 13. The normalization would correspond to an absolute spectroscopic factor of about 0.01. It is of course probable that this weak transition proceeds by some sort of multistep process, but a CCBA analysis was not attempted since simple two-step processes leading to an  $\frac{11}{2}^+$  state appear rather unlikely.

Although it is believed that all of these transitions indeed proceed primarily by two (or more) steps, the fact that the CCBA predictions in Fig. 13 may be closer to the data than the one-step predictions can hardly be taken as proof of the two-step mechanism at this level of analysis. Small amounts of one-step interference can also have large effects.<sup>21,24</sup>

Although absolute spectroscopic factors are quite sensitive to the deuteron potentials employed in these calculations, it is possible to give *relative* spectroscopic factors for states with known or probable assignments observed in this work. These should be reasonably accurate if the DWBA formulation is meaningful, assuming further that the  $Q$  dependence of the DWUCK predictions is

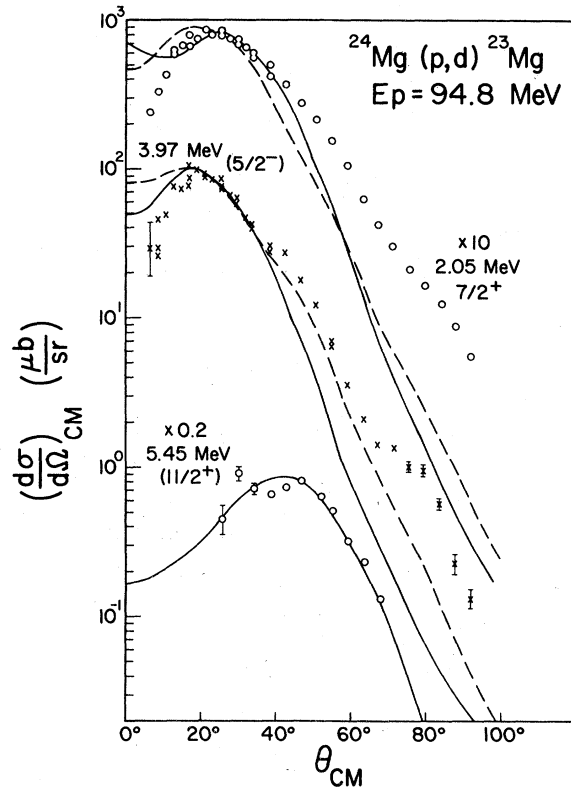


FIG. 13. Comparison of experimental data with normalized one-step DWBA predictions (shown by solid curves) and preliminary two-step CCBA predictions (shown by dashed curves) for the 2.05-MeV, 3.97-MeV, and 5.45-MeV states of  $^{23}\text{Mg}$ . The data for the 2.05-MeV and 5.45-MeV states were multiplied by the factors shown before plotting.

reliable.

Table II summarizes experimental spectroscopic factor and peak cross-section results for  $^{23}\text{Mg}$  from the present work at 94.8 MeV, spectroscopic factor results from earlier  $(p, d)$  studies by Kozub<sup>41</sup> at 33.6 MeV and by Källne and Fagerström<sup>5</sup> at 185 MeV, and available theoretical comparisons. Shell-model wave functions for the even parity states of  $A=23$  nuclei have been calculated recently by Chung and Wildenthal<sup>31</sup> in the full  $2s-1d$  shell basis space. The two-body matrix elements used in their calculations were treated as independent free parameters adjusted to fit experimental ground-state binding energies and level spacings. Their predictions for the energies and spectroscopic factors of the first two or three even-parity states of each spin are also shown in the top part of Table II. The predicted binding energies (with respect to  $^{16}\text{O}$ ) were normalized in the table so that the first predicted  $\frac{3}{2}^+$  state is the ground state of  $^{23}\text{Mg}$ . Since no shell-model predictions are available to our knowledge for  $A=23$

TABLE II. Comparisons of experimental and theoretical excitation energies and relative spectroscopic factors for states observed in present and previous ( $p, d$ ) experiments.

$^{23}\text{Mg}$ state $E_x$ (MeV)	$J^\pi$	$E_p = 33.6 \text{ MeV}^a$				$E_p = 185 \text{ MeV}^b$				$E_p = 94.8 \text{ MeV}$				Theoretical predictions			
		S <sub>1</sub>		S/S <sub>1</sub>		S <sub>1</sub>		S/S <sub>1</sub>		First maximum $\frac{d\sigma}{d\Omega}$ ( $\mu\text{b}/\text{sr}$ )		$\theta_{\text{c.m.}}$ (deg)		$E_x$ (MeV)		S <sub>1</sub>	S/S <sub>1</sub>
		S <sub>1</sub>	S/S <sub>1</sub>	S <sub>1</sub>	S/S <sub>1</sub>	S <sub>1</sub>	S/S <sub>1</sub>	S <sub>1</sub>	S/S <sub>1</sub>	$\theta_{\text{c.m.}}$	$\frac{d\sigma}{d\Omega}$	S <sub>1</sub>	S/S <sub>1</sub>	S <sub>1</sub>	S/S <sub>1</sub>	S <sub>1</sub>	S/S <sub>1</sub>
2.359	1st $\frac{1}{2}^+$	0.20	1.0	0.30	1.0	0.026	1.0	118	18.5 <sup>f</sup>	0.026	1.0	118	18.5 <sup>f</sup>	2.144	0.655	1.0	1.0
4.356	2nd $\frac{1}{2}^+$	0.72	0.5	0.58	0.40	0.24	0.70	86	18 <sup>f</sup>	0.24	0.70	86	18 <sup>f</sup>	4.371	0.278	0.42	0.42
0.000	1st $\frac{3}{2}^+$	5.66	1.0	5.80	1.0	1.14	1.0	955	8	1.14	1.0	955	8	0.000 <sup>g</sup>	0.409	1.0	1.0
2.908	(2nd $\frac{3}{2}^+$ )				0.655		0.71		11		0.71		11	2.831	0.647	1.58	1.58
0.451	1st $\frac{5}{2}^+$				1.0		1.0		Not observed		1.0		Not observed	0.387	4.809	1.0	1.0
3.863	(2nd $\frac{5}{2}^+$ )				0.095		0.140				0.140			3.699	0.002	$4 \times 10^{-5}$	$4 \times 10^{-5}$
5.285	(3rd $\frac{5}{2}^+$ )				0.107		0.140				0.140			5.409	0.769	0.160	0.160
2.051	1st $\frac{7}{2}^+$						1.0		23	0.028 <sup>g</sup>	1.0	82	23	2.154			
4.681	(2nd $\frac{7}{2}^+$ )						0.50 <sup>g</sup>		21.5	30	0.50 <sup>g</sup>	30	21.5	4.694			
2.715	(1st $\frac{9}{2}^+$ )								Not resolved			Not resolved	Not resolved	2.765			
5.450	1st $\frac{11}{2}^+$ ?								47?	4.0?	0.008 <sup>g</sup>	4.0?	47?	5.641			
2.771	1st $\frac{1}{2}^-$	3.40		22.0		2.42		>4760	<6.5	2.42		>4760	<6.5	2.771 <sup>h</sup>	2.863	1.0	1.0
3.795	1st $\frac{3}{2}^-$	1.69	1.0	5.4	1.0	0.69	1.0	>1800	<6.5	0.69	1.0	>1800	<6.5	4.701	0.003	0.001	0.001
5.986	(2nd $\frac{3}{2}^-$ )				0.667		0.61		>1310		0.61		>1310	5.751	0.645	0.225	0.225
8.91	( $\frac{5}{2}^-$ )								<6.5				<6.5	3.795 <sup>h</sup>	1.342	1.0	1.0
9.02	( $\frac{7}{2}^-$ )				0.104				<6.5				<6.5	5.975	0.072	0.054	0.054
									<8.6		0.09		<8.6	6.925	1.019	0.759	0.759
									<8.6		0.05		<8.6	8.275	1.798	1.340	1.340
														8.445	0.261	0.194	0.194
														9.235	0.123	0.092	0.092
														9.395	0.087	0.065	0.065
														10.055	0.058	0.043	0.043
9.67	( $\frac{9}{2}^-$ )				0.15-0.30		0.20	>421	<8.6		0.20	>421	<8.6	10.295	0.018	0.013	0.013
10.57	( $\frac{11}{2}^-$ )				0.11-0.19		0.13	>306	<8.6		0.13	>306	<8.6	10.565	0.280	0.209	0.209
														11.075	0.211	0.157	0.157
														11.395	0.026	0.019	0.019
														11.565	0.101	0.075	0.075
3.974	(1st $\frac{5}{2}^-$ )			94		0.019 <sup>g</sup>			19.5	94	0.019 <sup>g</sup>		19.5	11.775	0.240	0.179	0.179
														...	...	...	...

<sup>a</sup>Reference 41.<sup>b</sup>Reference 5.<sup>c</sup>Reference 31.<sup>d</sup>Reference 32.<sup>e</sup>Normalized to experimental excitation energy of low-

est state of this spin and parity.

<sup>f</sup>First observed maximum, true first maximum <6.5°.<sup>g</sup>Assuming (unlikely) pure one-step transition for comparison purposes.<sup>h</sup>A=27 predictions<sup>d</sup><sup>i</sup>A=23 predictions<sup>c</sup>

negative-parity states, the results of Maripuu<sup>32</sup> for *relative* excitation energies and spectroscopic factors of  $\frac{1}{2}^-$  and  $\frac{3}{2}^-$  states excited in  $^{28}\text{Si}(p, d)^{27}\text{Si}$  are included, even though any direct comparison with  $^{23}\text{Mg}$  is unrealistic. The work by Maripuu used the Oak Ridge shell-model code with realistic two-body interactions, and incorporated  $1p$  states as well as the  $s$ - $d$  states in the model space. Predicted excitation energies for  $^{27}\text{Si}$  were arbitrarily normalized in Table II to the lowest  $\frac{1}{2}^-$  and  $\frac{3}{2}^-$  states in  $^{23}\text{Mg}$ .

For general information only, included from the present work in Table II are the absolute spectroscopic factors ( $S_1$ ) for the lowest state of each spin and parity determined in a DWUCK calculation using the deuteron potential of Ref. 56. Since the extracted absolute spectroscopic factors depend strongly on the choice of deuteron potential, the relative spectroscopic factors ( $S/S_1$ ) for each spin and parity provide much more meaningful comparisons. An indication of relative spectroscopic factors for states of different spin and parity can be obtained from the table, since the absolute values of  $S_1$  for each spin and parity obtained with the same DWUCK parameters are given. However, the same deuteron potential was used in every case, which is not quite realistic because of the 10-MeV range of residual excitation energies covered in the table.

It should be emphasized that in the table spin-parity assignment entries without parentheses or question marks are the definite assignments of Endt and van der Leun.<sup>49</sup> Entries in parentheses are considered here to be very probable based upon the evidence available from this experiment, the mirror nucleus  $^{23}\text{Na}$ , and the shell-model calculations. It has also been assumed that only the lowest  $l=1$  group leads to a state with spin and parity  $\frac{1}{2}^-$ , based upon the results of Breuer *et al.*<sup>60</sup> for  $(d, ^3\text{He})$  analyzing powers in the  $s$ - $d$  shell. Question marks by entries indicate possible assignments only.

Examination of the even-parity states in Table II shows reasonable agreement between the present experiment and theory for the relative spectroscopic factors of the  $1d_{5/2}$  and  $2s_{1/2}$  transitions (although the latter are less reliable because of the poorer quality of the fits). The relative strengths of the two  $1d_{3/2}$  transitions are inverted compared to the theoretical prediction<sup>31</sup>; this is also the case for the 185-MeV measurements.<sup>5</sup>

The relative spectroscopic factors for the  $\frac{3}{2}^-$  states including the deep-hole states are qualitatively consistent with the  $^{27}\text{Si}$  expectations. Unresolved  $p_{3/2}$  strength no doubt occurs in some of the groups shown in Figs. 7 and 8, and in the clumps of states between 6.6 and 8.5 MeV or above

10.75 MeV, shown in Fig. 1. For this reason, reconstruction of an experimental  $(1p_{3/2})^{-1}$  quasihole structure<sup>36,61</sup> has not yet been attempted.

Comparisons in Table II with the previous experimental results for the *ratios* of spectroscopic factors in the few cases available generally show reasonable agreement at the bombarding energies of 33.6, 94.8, and 185 MeV. The largest deviations are for the  $2s_{1/2}$  transitions, where the quality of the DWBA fits is in fact the worst and the contributions to the predictions from the nuclear interior are the greatest.

## V. SUMMARY AND CONCLUSIONS

This study has examined for the first time with good resolution and large momentum transfer the high-excitation region of the residual nucleus from a  $(p, d)$  reaction on an  $s$ - $d$  shell target. From angular distributions obtained for the  $^{24}\text{Mg}(p, d)$  reaction at 94.8-MeV bombarding energy, it was possible to identify four deep-hole  $p$  states at excitations of 8.91, 9.02, 9.67, and 10.57 MeV in  $^{23}\text{Mg}$ . From shell-model calculations<sup>32</sup> for the nearby nucleus  $^{27}\text{Si}$ , these are presumed to be fragmented states from the  $1p_{3/2}$  shell.

Angular distributions were also obtained for 29 other deuteron groups leading to states (or groups of unresolved states) up to 10.75-MeV excitation in  $^{23}\text{Mg}$ . The excitation energies determined are in good agreement with the compilation of Endt and van der Leun<sup>49</sup> up to 7.25 MeV and the  $^{25}\text{Mg}(p, t)^{23}\text{Mg}$  work of Nann *et al.*<sup>43</sup> up to 9.72 MeV. Above 9.72 MeV, excitation energies for 18 deep-hole states (or groups of states) were obtained up to 13.28 MeV.

Characteristic angular distribution signatures are found for known  $l=0$  transitions (strong oscillations) and transitions which must proceed primarily by two-step processes (broad maxima with no oscillations). Except at the very forward angles ( $6^\circ$  to  $10^\circ$  in the laboratory system),  $l=1$  and  $l=2$  transitions are very similar and drop exponentially with large momentum transfer with very minor oscillations superimposed.  $l=1$  and  $l=2$  states were best differentiated by an empirical method which removed the exponential momentum transfer ( $q$ ) dependence by dividing by  $\exp(-q/66 \text{ MeV}/c)$ , or a plane-wave theoretical approach which multiplied the observed cross sections by  $(q^2 + \kappa^2)^2$ , where  $\kappa^2$  is directly determined from the neutron separation energy. Both methods give distinctive maxima at low momentum transfers, at about 115 MeV/ $c$  for  $l=1$  and 155 MeV/ $c$  for  $l=2$  transitions.

Empirical analyses of the angular distributions, coupled with information from the mirror nucleus

$^{23}\text{Na}$  and other experimental evidence, lead to very probable assignments of  $\frac{5}{2}^-$  to the 3.97-MeV state of  $^{23}\text{Mg}$  and  $\frac{7}{2}^+$  to the 4.68-MeV state. The results are also consistent with (but do not prove) a  $\frac{9}{2}^+$  assignment to the 2.71-MeV state, and an  $\frac{11}{2}^+$  assignment for the 5.45-MeV state.

DWBA predictions using existing proton and deuteron potentials show rather good agreement in the shape of the angular distributions only for the  $l=2$  transitions, which have little contribution from the nuclear interior; however, absolute  $l=2$  spectroscopic factors vary by up to a factor of 3 for different deuteron potentials.  $l=0$  transitions are not fit in either slope or locations of the oscillatory maxima or minima. Preliminary two-step CCBA predictions for transitions to the  $\frac{7}{2}^+$  state of  $^{23}\text{Mg}$  at 2.05 MeV and the probable  $\frac{5}{2}^-$  state at 3.97 MeV agree about as well with the data as the DWBA predictions for other known one-step transitions. Relative spectroscopic factors for known one-step transitions are in reasonable agreement with detailed shell-model calculations by Chung and Wildenthal,<sup>31</sup> and by Maripuu.<sup>32</sup>

The major difficulty with the DWBA ( $p, d$ ) predictions compared to ( $d, t$ ) may be a consequence of the long proton mean free path.<sup>62</sup> At the same time the present results may present a new opportunity to study the nuclear interior, since it is likely that ( $p, d$ ) processes can occur there at these energies. Difficulties in DWBA analyses to date may be due to the fact that deuteron wave functions derived from elastic scattering are not accurate in the nuclear interior. Such an interpretation is consistent with the fact that the worst one-step fits in this work are obtained for the  $l=0$  transitions, which also show significant contributions to the predicted cross sections from well inside the nuclear radius.

It should finally be emphasized that the DWBA predictions in this work were straightforward DWUCK calculations<sup>54</sup> with standard finite-range

and nonlocality corrections, and used available optical potentials from the literature. No attempt was made to investigate all possible alternatives and corrections to the DWBA in detail prior to publishing these experimental results, since the primary motivation for this work was the location and  $l$  assignments for the prominent deep-hole states. Further, a very recent detailed DWBA study by Anderson *et al.*<sup>17</sup> has been made of ( $p, d$ ) reactions in heavier nuclei at a similar bombarding energy.

#### ACKNOWLEDGMENTS

We would like to acknowledge the theoretical assistance of Professor G. E. Walker at all stages of this experiment. Professor R. E. Pollock, Professor V. C. Officer (Melbourne), and Dr. R. E. Kouzes made important contributions in the early stages of the experimental setup for ( $p, d$ ) experiments at IUCF. Dr. S. Maripuu provided not only his shell-model calculations for  $A=27$  nuclei, but also detailed assistance in their interpretation. Special thanks are due to Dr. H. Nann (Northwestern) for providing the results of the Michigan State  $^{25}\text{Mg}(p, t)^{23}\text{Mg}$  experiments prior to publication, and for discussions and analysis of the implications of that work. Professor B. H. Wildenthal (Michigan State) also very kindly provided the results of detailed shell-model calculations for  $A=23$  nuclei. Valuable discussions with Professor J. R. Shepard (Colorado), Dr. R. E. Anderson (LAMPF), and Dr. G. S. Adams (LAMPF) were also appreciated. The assistance of J. Meek, K. Hicks, and C. Lane in data analysis, of W. Lozowski in target preparation, and of the entire operations staff of the Indiana University Cyclotron Facility is gratefully acknowledged.

This work was supported in part by National Science Foundation Grant No. PHY 76-84033.

\*Present address: TRIUMF, University of British Columbia, Vancouver, B. C., V6T 1W5 Canada.

<sup>1</sup>M. Sakai and K. I. Kubo, Nucl. Phys. **A185**, 217 (1972).

<sup>2</sup>T. Ishimatsu, S. Hayashibe, N. Kawamura, T. Awaya, H. Ohmura, Y. Nakajima, and S. Mitarai, Nucl. Phys. **A185**, 273 (1972).

<sup>3</sup>J. Källne and B. Fagerström, in *Proceedings of the Fifth International Conference on High Energy Physics and Nuclear Structure*, edited by G. Tibell (North-Holland, Amsterdam, 1974), p. 369.

<sup>4</sup>B. Fagerström and J. Källne, Phys. Scr. **8**, 14 (1973).

<sup>5</sup>J. Källne and B. Fagerström, Phys. Scr. **11**, 79 (1974).

<sup>6</sup>J. Källne, V. Gustaf Werner Institute, Internal Report No. G.W.I./P.H., 1975 (unpublished).

<sup>7</sup>M. Sakai, M. Sekiguchi, F. Soga, Y. Hirao, K. Yagi, and Y. Aoki, Phys. Lett. **51B**, 51 (1974).

<sup>8</sup>E. Gerlic, H. Langevin-Joliot, P. Roos, J. Van de Wiele, J. P. Didelez, and G. Duhamel, Phys. Rev. **C 12**, 2106 (1975).

<sup>9</sup>E. Gerlic, J. Källne, H. Langevin-Joliot, J. Van de Wiele, and G. Duhamel, Phys. Lett. **57B**, 338 (1975).

<sup>10</sup>G. J. Wagner, G. Mairle, and U. Schmidt-Rohr, Nucl. Phys. **A125**, 80 (1969).

<sup>11</sup>E. Krämer, G. Mairle, and G. Kaschl, Nucl. Phys. **A165**, 353 (1971).

<sup>12</sup>M. Arditi, L. Bimbot, H. Doubre, N. Frascaria, J. P. Garron, M. Rofu, and D. Royer, Nucl. Phys. **A165**, 129 (1971).

<sup>13</sup>S. Y. van der Werf, B. R. Kooistra, W. H. A. Hesse-



- link, F. Iachello, L. W. Put, and R. H. Siemssen, *Phys. Rev. Lett.* **33**, 712 (1974).
- <sup>14</sup>G. J. Wagner, in *Proceedings of the International Symposium on Highly Excited States in Nuclei, Jülich, 1975*, edited by A. Faessler, C. Mayer-Böricke, and P. Turek (KFA Jülich, W. Germany, 1975), Vol. 2, p. 177.
- <sup>15</sup>S. D. Baker, R. Bertini, R. Beurtey, F. Brochard, G. Bruge, H. Catz, A. Chaumeaux, G. Crijanovich, J. M. Durand, J. C. Faivre, J. M. Fontaine, D. Garreta, F. Hibou, D. Legrand, J. C. Lugol, J. Sandinos, J. Thirion, and E. Rost, *Phys. Lett.* **52B**, 57 (1974).
- <sup>16</sup>E. Rost and J. W. Shepard, *Phys. Lett.* **59B**, 413 (1975).
- <sup>17</sup>R. E. Anderson, J. J. Kraushaar, J. R. Shepard, and J. R. Comfort, *Nucl. Phys.* **A311**, 93 (1978).
- <sup>18</sup>G. J. Igo, *Rev. Mod. Phys.* **50**, 523 (1978).
- <sup>19</sup>W. T. Pinkston and G. R. Satchler, *Nucl. Phys.* **72**, 641 (1965).
- <sup>20</sup>E. Rost, *Phys. Rev.* **154**, 994 (1967).
- <sup>21</sup>J. Källne and A. W. Obst, *Phys. Rev. C* **15**, 477 (1977).
- <sup>22</sup>P. G. Roos, S. M. Smith, V. K. C. Cheng, G. Tibell, A. A. Cowley, and R. A. J. Riddle, *Nucl. Phys.* **A255**, 187 (1975).
- <sup>23</sup>J. N. Craig, N. S. Wall and R. H. Bassel, *Phys. Rev. Lett.* **36**, 656 (1976).
- <sup>24</sup>J. R. Shepard, R. E. Anderson, J. J. Kraushaar, and J. R. Comfort, University of Colorado Nuclear Physics Laboratory Technical Progress Report No. NPL-793, 1977 (unpublished), p. 123.
- <sup>25</sup>G. R. Smith, J. R. Shepard, R. L. Boudrie, R. J. Peterson, N. J. DiGiacomo, J. J. Kraushaar, G. Igo, C. A. Whitten, T. S. Bauer, G. Adams, and G. Pauletta, University of Colorado Nuclear Physics Laboratory Technical Progress Report No. NPL-816, 1978 (unpublished), p. 135.
- <sup>26</sup>C. A. Whitten, Jr., G. Adams, T. S. Bauer, G. Igo, G. Pauletta, A. Wriekat, R. L. Boudrie, J. R. Shepard, G. R. Smith, G. W. Hoffmann, and B. Hoistad, *Bull. Am. Phys. Soc.* **23**, 934A (1978).
- <sup>27</sup>D. W. Miller, D. W. Devins, R. E. Pollock, and R. Kouzes, *Bull. Am. Phys. Soc.* **21**, 978A (1976).
- <sup>28</sup>Indiana University Cyclotron Facility Technical and Scientific Report, Nov. 1975 to Jan. 1977 (unpublished), p. 37.
- <sup>29</sup>G. S. Adams, A. D. Bacher, G. T. Emery, W. P. Jones, R. T. Kouzes, D. W. Miller, A. Pickelsimer, and G. E. Walker, *Phys. Rev. Lett.* **38**, 1387 (1977).
- <sup>30</sup>B. M. Spicer, D. W. Devins, D. L. Friesel, W. P. Jones, A. C. Attard, V. C. Officer, G. G. Shute, I. D. Svalbe, R. S. Henderson, and S. F. Collins, Research Proposal to the Indiana University Cyclotron Facility, 1978 (unpublished).
- <sup>31</sup>W. Chung and B. H. Wildenthal, Michigan State University (private communication).
- <sup>32</sup>S. Maripuu (private communication).
- <sup>33</sup>M. Sekiguchi, Y. Shida, F. Soga, T. Hattori, Y. Hirao, and M. Sakai, *Phys. Rev. Lett.* **38**, 1015 (1977).
- <sup>34</sup>R. H. Siemssen, in *Proceedings of the International Conference on Nuclear Structure, Tokyo, 1977*, *J. Phys. Soc. Jpn.* **44**, Suppl. p. 137 (1978).
- <sup>35</sup>P. K. Bindal, D. H. Youngblood, and R. L. Kozub, *Phys. Rev. C* **10**, 729 (1974); P. K. Bindal, D. H. Youngblood, R. L. Kozub, and P. H. Hoffmann-Pinther, *ibid.*, **12**, 390 (1975).
- <sup>36</sup>P. Doll, G. J. Wagner, K. T. Knöpfle, and G. Mairle, *Nucl. Phys.* **A263**, 210 (1976).
- <sup>37</sup>T. Koeling and F. Iachello, *Nucl. Phys.* **A295**, 45 (1978).
- <sup>38</sup>W. W. Jacobs, S. E. Vigdor, W. P. Jones, R. E. Marrs, and D. W. Miller, *Bull. Am. Phys. Soc.* **23**, 539A (1978).
- <sup>39</sup>Indiana University Cyclotron Facility Technical and Scientific Report, Feb. 1977 to Jan. 1978 (unpublished), p. 48.
- <sup>40</sup>C. D. Kavaloski, G. Bassani, and N. M. Hintz, *Phys. Rev.* **132**, 813 (1963).
- <sup>41</sup>R. L. Kozub, *Phys. Rev.* **172**, 1078 (1968).
- <sup>42</sup>P. D. Kunz, E. Rost, and R. R. Johnson, *Phys. Rev.* **177**, 1737 (1969).
- <sup>43</sup>H. Nann, A. Saha, and K. K. Seth, Michigan State University (private communication).
- <sup>44</sup>D. W. Miller, W. P. Jones, R. E. Marrs, and D. W. Devins, *Bull. Am. Phys. Soc.* **23**, 527A (1978). Also Ref. 39, p. 58.
- <sup>45</sup>Reference 28, pp. 16, 22-24; also R. D. Bent, D. G. Madland, J. D. Cossairt, A. D. Bacher, W. P. Jones, D. W. Miller, R. E. Pollock, and P. Schwandt, Indiana University Cyclotron Facility Report No. 1-73, 1973 (unpublished).
- <sup>46</sup>V. C. Officer, R. S. Henderson, and I. D. Svalbe, *Bull. Am. Phys. Soc.* **20**, 1169A (1975).
- <sup>47</sup>R. Kouzes, *Bull. Am. Phys. Soc.* **21**, 1006A (1976).
- <sup>48</sup>R. B. Hindsley and J. T. Meek, Indiana University Cyclotron Facility (private communication).
- <sup>49</sup>P. M. Endt and C. van der Leun, *Nucl. Phys.* **A310**, 1 (1978).
- <sup>50</sup>R. O. Nelson and N. R. Roberson, *Phys. Rev. C* **6**, 2153 (1972).
- <sup>51</sup>J. Dubois and L. G. Earwaker, *Phys. Rev.* **160**, 925 (1967).
- <sup>52</sup>R. D. Amado and R. M. Woloshyn, *Phys. Lett.* **62B**, 253 (1976).
- <sup>53</sup>For example, M. A. Preston, *Physics of the Nucleus* (Addison Wesley, Reading, Mass., 1962), pp. 571-575.
- <sup>54</sup>P. D. Kunz, University of Colorado (private communication).
- <sup>55</sup>A. Nadasen, P. Schwandt, P. P. Singh, A. D. Bacher, P. T. Debevec, W. W. Jacobs, M. D. Kaitchuck, and J. T. Meek, *Phys. Rev. C* (to be published).
- <sup>56</sup>A. Kiss, O. Aspelund, G. Hrehuss, K. T. Knöpfle, M. Rogge, U. Schwinn, Z. Seres, P. Turek, and C. Mayer-Böricke, *Nucl. Phys.* **A262**, 1 (1976).
- <sup>57</sup>G. Duhamel, L. Marcus, H. Langevin-Joliot, J. P. Didelez, P. Narboni, and C. Stephen, *Nucl. Phys.* **A174**, 485 (1971).
- <sup>58</sup>R. C. Johnson, and P. J. R. Soper, *Phys. Rev. C* **1**, 976 (1970).
- <sup>59</sup>A. Moalem, J. F. A. Van Hienen, and E. Kashy, *Nucl. Phys.* **A307**, 277 (1978).
- <sup>60</sup>H. Breuer, P. Doll, K. T. Knöpfle, G. Mairle, H. Riedesel, K. Schindler, G. J. Wagner, V. Bechtold, and L. Friedrich, Annual Report, Max Planck Institut für Kernphysik, Heidelberg, 1977, pp. 98-100.
- <sup>61</sup>G. J. Wagner, P. Doll, K. T. Knöpfle and G. Mairle, *Phys. Lett.* **57B**, 413 (1975).
- <sup>62</sup>J. C. Peng, H. S. Song, F. C. Wang, and J. V. Maher, *Phys. Rev. Lett.* **41**, 225 (1978).